

Reentrant topological transitions with Majorana end states in one-dimensional superconductors by lattice modulation

Masaki Tezuka* and Norio Kawakami

Department of Physics, Kyoto University, Kyoto 606-8502, Japan

(Received 4 August 2013; published 21 October 2013)

The possibility to observe and manipulate Majorana fermions as end states of one-dimensional topological superconductors has been actively discussed recently. In a quantum wire with strong spin-orbit coupling placed in proximity to a bulk superconductor, a topological superconductor has been expected to be realized when the band energy is split by the application of a magnetic field. When a periodic lattice modulation is applied, multiple topological superconductor phases appear in the phase diagram. Some of them occur for higher filling factors compared to the case without the modulation. We study the effects of phase jumps and argue that the topologically nontrivial state of the whole system is retained even if they are present. We also study the effect of the spatial modulation in the hopping parameter.

DOI: [10.1103/PhysRevB.88.155428](https://doi.org/10.1103/PhysRevB.88.155428)

PACS number(s): 74.90.+n, 71.10.Pm, 03.65.Vf, 67.85.-d

I. INTRODUCTION

Much work has been devoted to realize topologically nontrivial states of matter with topologically protected surface states. Majorana surface states are expected to be formed at the boundaries and vortex cores of topological superconductors (TSs).¹⁻⁷ Such states have been expected in a one-dimensional (1D) quantum wire with spin-orbit interaction (SOI) placed under a Zeeman field and in proximity to a bulk superconductor,⁸⁻¹¹ in cold atoms in optical lattices with effective gauge fields generated by spatially varying laser fields,⁶ bilayer electron gases in a semiconductor heterostructure with interlayer Coulomb coupling,¹² among others. Several groups of experimentalists have recently reported that they have observed the signatures of Majorana fermions appearing at the ends of nanowires attached to superconductors.¹³⁻¹⁶ For a review we refer to Ref. 17.

The effect of spatial inhomogeneity on a superconducting quantum wire has been a nontrivial problem.¹⁸⁻²⁶ The energy distributions of the end states have been obtained for the Dirac equation with random mass and a 1D spinless superconductor.²⁰ The interplay of disorder and correlation in 1D TSs has also been investigated.²² Among the possible realizations of spatial inhomogeneity, quasiperiodic (Harper) potential modulation²⁷ forms a special class in that in a 1D system all the single particle eigenstates become localized at the same modulation strength. Quasiperiodic potentials have been experimentally studied in optically trapped cold atom systems²⁸ as well as in solid state, misfit compound²⁹ systems. Signatures of a Hofstadter butterflylike band structure have been observed in a van der Waals system of monolayer graphene on top of a hexagonal boron nitride surface.³⁰

The 1D effective spinless superconductor, expected in 1D superconductors with strong spin-momentum coupling under magnetic field, is of the D symmetry class.³¹ Therefore its topology is classified by a Z_2 topological number. This suggests that the boundary between two topologically nontrivial 1D superconductors would not have a localized mode. Boundary phenomena between topologically equivalent or distinct phases, with Harper or Fibonacci potentials, have been experimentally studied using photonic quasicrystals.³²

In the scenario of Refs. 8–11 the chemical potential needs to lie close to the band edge so that the band degeneracy is removed by the external magnetic field. However, the present authors have observed that, by a quasiperiodic lattice modulation with a fixed wave number, an effective single-band superconductor with end Majorana fermions is realized even when the chemical potential is closer to the center of the original cosine band, because energy separations are introduced within each of the Zeeman-split bands.³³ We have also demonstrated that this physics is stable even in the presence of a Hubbard-like on-site interaction and/or a harmonic trapping potential. More recently, the effect of incommensurate potentials on 1D p -wave superconductors have been studied.³⁴⁻³⁶ Commensurate diagonal or off-diagonal Harper models,^{37,38} and the effect of a spatially varying component of the magnetic field,³⁹ have also attracted theoretical attention.

Here we are interested in further characterizing the new TS regions, focusing on when they emerge, and what happens when the quasiperiodically modulated quantum wire is connected with other wires with different modulation phases or an unmodulated one. Particularly, we would like to (i) clarify the correspondence between the energy spectrum of the single particle states and the emergence of the TS states, in the presence of either a quasiperiodic modulation with a general wave number or the external magnetic field to a general direction, (ii) understand the effect of phase jumps of the quasiperiodic modulation and that of a quasiperiodic modulation applied to only a limited part of the one-dimensional system, and (iii) study the effect of a quasiperiodic modulation of the hopping parameter.

In Sec. II we define our model and introduce our Bogoliubov–de Gennes (BdG) equation approach to study the system. We find that with a lattice-site energy modulation with a generic wave number, quasiperiodic or periodic, new topological superconducting regions with end Majorana fermions emerge. We also study the effect of the direction of the external magnetic field. Then in Sec. III we observe that those regions are stable against phase jumps in one-dimensional systems, while when the modulated wire is connected with an unmodulated wire, the locations of the localized modes are determined by which of the wires becomes TS. We also study

the case with quasiperiodic modulation in the intersite hopping parameter, and find that multiple topological transitions into and out of TS states occur. Finally, in Sec. IV, we summarize our findings.

II. SITE LEVEL MODULATION BY A SINGLE (QUASI)PERIODIC LATTICE POTENTIAL

We consider a one-dimensional quantum wire parallel to the \hat{x} direction, coupled to a bulk superfluid whose surface is perpendicular to \hat{z} . We study a tight-binding one-dimensional model of spin-1/2 fermions with the Rashba-type spin-orbit coupling, the mean-field coupling to the bulk superconductor, and the Zeeman energy due to the external magnetic field \mathbf{B} .

The Hamiltonian we have adopted is

$$\begin{aligned} \mathcal{H} = & -\frac{t}{2} \sum_{l=0}^{L-2} \sum_{\sigma=\uparrow,\downarrow} (\hat{c}_{\sigma,l}^\dagger \hat{c}_{\sigma,l+1} + \text{H.c.}) \\ & + \frac{\alpha}{2} \sum_{l=0}^{L-2} [(\hat{c}_{\downarrow,l}^\dagger \hat{c}_{\uparrow,l+1} - \hat{c}_{\uparrow,l}^\dagger \hat{c}_{\downarrow,l+1}) + \text{H.c.}] \\ & + \sum_{l=0}^{L-1} \left[\Delta (\hat{c}_{\uparrow,l} \hat{c}_{\downarrow,l} + \text{H.c.}) + \frac{2\Gamma}{\hbar} \hat{\mathbf{B}} \cdot \mathbf{S}_l \right] \\ & + \sum_{l=0}^{L-1} \sum_{\sigma=\uparrow,\downarrow} (t - \mu + \epsilon_{\sigma,l}) \hat{n}_{\sigma,l}, \end{aligned} \quad (1)$$

with $\Gamma \equiv \frac{g\mu_B}{2} B$. We set $t = 1$ as the unit of energy and set $\hbar = 1$ in the following. In the case of $\hat{\mathbf{B}} = \hat{z}$ the third line becomes

$$\sum_{l=0}^{L-1} [\Delta (\hat{c}_{\uparrow,l} \hat{c}_{\downarrow,l} + \text{H.c.}) + \Gamma (\hat{n}_{\uparrow,l} - \hat{n}_{\downarrow,l})].$$

Here, $\hat{c}_{\sigma,l}$ annihilates a fermion with spin $\sigma (= \uparrow, \downarrow)$ at site $l (= 0, 1, \dots, L-1)$, $\hat{n}_{\sigma,l} \equiv \hat{c}_{\sigma,l}^\dagger \hat{c}_{\sigma,l}$, t determines the nearest-neighbor hopping, α is the Rashba-type SOI, Δ is the coupling to the bulk superconductor, Γ is the Zeeman energy, μ is the chemical potential, and $\epsilon_{\sigma,l}$ is the site energy for spin σ on site l .

In this paper we limit our discussion to the case with $\epsilon_{\sigma,l} = \epsilon_l$. In the following we introduce a quasiperiodic modulation to the site energy, and study the energy distribution of the single particle states and its correspondence with the realization of Majorana end modes. Here, the single particle Hamiltonian is obtained by setting $\Delta = \mu = 0$ in Eq. (1), as

$$\begin{aligned} \mathcal{H}_{\text{Single}} = & -\frac{t}{2} \sum_{l=0}^{L-2} \sum_{\sigma=\uparrow,\downarrow} (\hat{c}_{\sigma,l}^\dagger \hat{c}_{\sigma,l+1} + \text{H.c.}) \\ & + \frac{\alpha}{2} \sum_{l=0}^{L-2} [(\hat{c}_{\downarrow,l}^\dagger \hat{c}_{\uparrow,l+1} - \hat{c}_{\uparrow,l}^\dagger \hat{c}_{\downarrow,l+1}) + \text{H.c.}] \\ & + \sum_{l=0}^{L-1} \left[\frac{2\Gamma}{\hbar} \hat{\mathbf{B}} \cdot \mathbf{S}_l + \sum_{\sigma=\uparrow,\downarrow} (t + \epsilon_l) \hat{n}_{\sigma,l} \right]. \end{aligned} \quad (2)$$

A. Double Hofstadter butterfly

Let us first consider the case of $\hat{\mathbf{B}} = \hat{z}$. For an infinitely long system having $\Delta = \epsilon_l = 0$ we easily obtain the single particle energy as a function of the quasimomentum k ,

$$E^\pm(k) = t[1 - \cos(k)] \pm \sqrt{\alpha^2 \sin^2(k) + \Gamma^2}. \quad (3)$$

We call them the upper and lower Rashba-Zeeman (RZ) bands.³³ The mapping of the Hamiltonian to that of a spinless system is possible if μ lies in only one of the RZ bands.^{10,11,40} In such a case, by introducing the pairing Δ such that $|\Delta| \lesssim \Gamma$, we obtain the topological superconductor phase.

We consider a site potential which is given by

$$\epsilon_l = V_Q \cos[\kappa(l - l_c) + \phi_0], \quad (4)$$

in which $V_Q \geq 0$, $l_c \equiv (L-1)/2$, ϕ_0 is the phase of the potential at the center of the system, and $\kappa = 2\pi g$, in which g is a real number such that $0 < g < 1$. The potential is periodic for a rational g , while it is quasiperiodic for an irrational g . In the following we choose $\phi_0 = 0$, except when we study the effect of ϕ_0 and when we study the effect of phase jumps in the system.

In a finite length system with L lattice sites, we numerically obtain the set of single particle level energies. For $\alpha = \Gamma = 0$, each single body wave function is extended for $V_Q < t$ and localized for $V_Q > t$ in the $L \rightarrow \infty$ limit.⁴¹ The self-similar structure of the two-dimensional spectrum plotted against κ for $V_Q = t$ is called the Hofstadter butterfly.^{41,42}

When the $2L$ energy levels obtained are plotted against various values of κ , for $V_Q \sim t$, the spectrum shows a self-similar structure resembling two Hofstadter butterflies shifted in energy and braided together, as shown in Fig. 1. We call this structure the double Hofstadter butterfly.³³

The spin-orbit coupling α mixes the spin-up states and spin-down states differently at each value of the quasimomentum k of the resulting RZ bands. Therefore the spin-independent site potential, which has components with $|k| = \pm\kappa$ and $|k| = \pm(2\pi - \kappa)$, further mixes the upper and lower RZ bands. Most of the states in the resulting double Hofstadter butterfly do not have a completely polarized spin. We may, however, obtain the expectation value of the z component of the spin $\langle S_z \rangle$ for each of the $2L$ eigenstates. The energy levels plotted in Fig. 1 have been color coded according to the value of $\langle S_z \rangle$.

We find that, for a fixed value of κ , the sets of states from two Hofstadter-butterfly-like structures with separated values of spin polarizations overlap within some energy ranges. In some regions in energy there are no single particle states, even inside the range of $|\epsilon - t| \leq t + \Gamma$, which was occupied by states of Eq. (3) before the introduction of the site potential modulation Eq. (4). Other regions are occupied by states in only one of the Hofstadter-butterfly-like structures. We study the consequences of the site potential modulation on the realization of TS states for the many-body states with a finite chemical potential in the following.

B. Bogoliubov–de Gennes equation: Zero modes and Majorana fermions

The Hamiltonian (1) is bilinear in operators \hat{c} and \hat{c}^\dagger . It can be exactly diagonalized in the Nambu spinor space

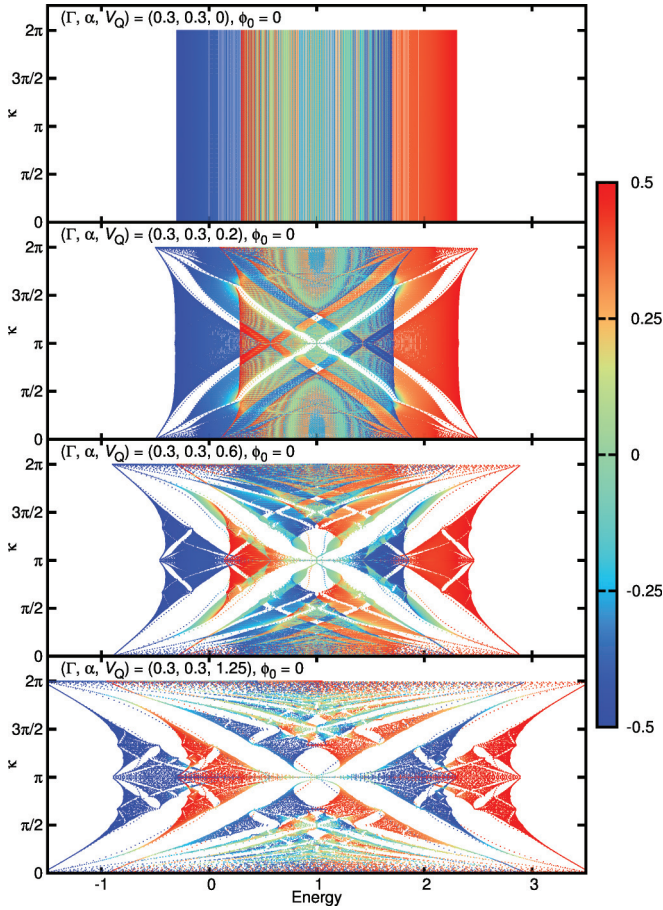


FIG. 1. (Color online) The distribution of single particle state energy of Eq. (2) for $L = 200$, $(\Gamma, \alpha) = (0.3, 0.3)$, $V_Q = 0, 0.2, 0.6, 1.25$, $\hat{\mathbf{B}} = \hat{z}$. The single particle Hamiltonian (2) is diagonalized for $\kappa = 2\pi j/400$ ($j = 0, 1, \dots, 400$) and each eigenstate is plotted in a color corresponding to the expectation value of the z component of the spin for that eigenstate. The plot for $V_Q = 1.25$ is similar to that for $V_Q = 0.8$ (not shown) except that the former is scaled horizontally, because of the duality of the lattice between $V_Q = x$ and $1/x$. $V_Q = 1$ is the self-similar point, at which the modulation potential equals the unmodulated bandwidth for $\Gamma = \alpha = 0$.

$\{(\mathbf{u}_\uparrow, \mathbf{u}_\downarrow, \mathbf{v}_\uparrow, \mathbf{v}_\downarrow)^T\}$, with the basis obtained as the set of the eigenvectors of the Bogoliubov–de Gennes (BdG) equation.

Alternatively, fermion pairing via a short-range attractive interaction can also be simulated by introducing a pairing constant g and solving the Bogoliubov–de Gennes equation self-consistently. In a lattice system the energy cutoff which renormalizes g can be in principle determined from the lattice constant. However, here we fix the value of Δ , a homogeneous proximity pairing, by hand. This is because we do not expect that the BdG approximation, which simulates the pair formation *within* the 1D wire, directly corresponds to our Hamiltonian (1).

We solve^{43,44}

$$\begin{pmatrix} \hat{H}_{\uparrow\uparrow} & \hat{H}_{\uparrow\downarrow} & 0 & \Delta \\ \hat{H}_{\downarrow\uparrow} & \hat{H}_{\downarrow\downarrow} & -\Delta & 0 \\ 0 & -\Delta & -\hat{H}_{\uparrow\uparrow} & -\hat{H}_{\uparrow\downarrow} \\ \Delta & 0 & -\hat{H}_{\downarrow\uparrow} & -\hat{H}_{\downarrow\downarrow} \end{pmatrix} \Psi = \epsilon \Psi, \quad (5)$$

in which $\Psi = (\mathbf{u}_\uparrow, \mathbf{u}_\downarrow, \mathbf{v}_\uparrow, \mathbf{v}_\downarrow)^T$ is a $4L$ -dimensional vector and $\hat{H}_{\sigma\sigma'}$ are the single particle components of the Hamiltonian,

$$\begin{aligned} \hat{H}_{\sigma\sigma} &= -\frac{t}{2} \sum_{l=0}^{L-2} \sum_{\sigma=\uparrow,\downarrow} (\hat{c}_{\sigma,l}^\dagger \hat{c}_{\sigma,l+1} + \text{H.c.}) \\ &+ \sum_{l=0}^{L-1} \sum_{\sigma=\uparrow,\downarrow} [t - \mu + \epsilon_l + (-)^\sigma (\hat{\mathbf{B}} \cdot \hat{\mathbf{z}}) \Gamma] \hat{n}_{\sigma,l}, \quad (6) \\ \hat{H}_{\downarrow\uparrow} &= \hat{H}_{\uparrow\downarrow}^\dagger = \frac{\alpha}{2} \sum_{l=0}^{L-2} (\hat{c}_{\downarrow,l}^\dagger \hat{c}_{\uparrow,l+1} - \hat{c}_{\downarrow,l+1}^\dagger \hat{c}_{\uparrow,l}) \\ &- [(\hat{\mathbf{B}} \cdot \hat{\mathbf{x}}) + i(\hat{\mathbf{B}} \cdot \hat{\mathbf{y}})] \Gamma \sum_{l=0}^{L-1} \hat{c}_{\downarrow,l}^\dagger \hat{c}_{\uparrow,l}, \quad (7) \end{aligned}$$

in which $(-)^{\sigma} = \delta_{\sigma\downarrow} - \delta_{\sigma\uparrow}$. In the following we call the $4L$ -dimensional matrix in the left hand side of Eq. (5) H_{BdG} .

We work in the limit of low temperature $T \rightarrow 0$. We obtain the particle distribution by

$$n_{\sigma,l} = \sum_q [f(\epsilon_q) |u_{\sigma,l}|^2 + f(-\epsilon_q) |v_{\sigma,l}|^2], \quad (8)$$

in which $f(\epsilon) \equiv [1 + e^{\epsilon/(k_B T)}]^{-1} \rightarrow \Theta(-\epsilon)$ ($T \rightarrow 0$) is the Fermi distribution function, with $\Theta(x)$ being the step function. The total number of fermions with spin σ is obtained as $N_\sigma = \sum_l n_{\sigma,l}$.

The sum in Eq. (8) is taken over all q . H_{BdG} is Hermitian, and has pairs of positive and negative eigenvalues with equal absolute values, because if $H_{\text{BdG}}(\mathbf{u}_\uparrow, \mathbf{u}_\downarrow, \mathbf{v}_\uparrow, \mathbf{v}_\downarrow)^T = \epsilon(\mathbf{u}_\uparrow, \mathbf{u}_\downarrow, \mathbf{v}_\uparrow, \mathbf{v}_\downarrow)^T$, we have $H_{\text{BdG}}(\mathbf{v}_\uparrow, \mathbf{v}_\downarrow, \mathbf{u}_\uparrow, \mathbf{u}_\downarrow)^T = -\epsilon(\mathbf{v}_\uparrow, \mathbf{v}_\downarrow, \mathbf{u}_\uparrow, \mathbf{u}_\downarrow)^T$. For a positive (negative) eigenvalue, only $|v_{\sigma,l}|^2$ ($|u_{\sigma,l}|^2$) contributes to the particle distribution in the $T \rightarrow 0$ limit.

1. Distribution of eigenvalues

For L sites in the system, because of the spin and particle-hole degrees of freedom, we have $4L$ eigenstates of the BdG equation (5). The introduction of Δ opens a gap in the eigenvalue spectrum of Eq. (5) in the absence of the spin-orbit coupling α or the Zeeman field Γ . With the spin-orbit coupling and the Zeeman field, when the chemical potential μ satisfies

$$(\text{lower band bottom}) < \mu < (\text{upper band bottom})$$

so that the Kitaev model² is effectively realized in the spinful case, the system is a topological superconductor for $0 < \Delta \lesssim \Gamma$ when \mathbf{B} is in the z - x plane.^{8–11,17} In this case the BdG equation has two eigenstates with $\epsilon \sim 0$.

Let us consider the $(2L)$ th and $(2L+1)$ th smallest eigenvalues, ϵ^- and ϵ^+ , which satisfy $-\epsilon^- = \epsilon^+$ because eigenvalues appear in pairs with the same absolute value and opposite signs, as mentioned above. We can only have an even number of vanishing eigenvalues, and if we have them ϵ^- and ϵ^+ should be included in them, otherwise $\epsilon^- < 0 < \epsilon^+$.

For $\mu \ll \{-t, \min(\epsilon_l)\}$, the number of fermions in the system is negligible. As μ is increased, N_σ increases, with $N_\downarrow > N_\uparrow$ for $\Gamma > 0$. ϵ^+ initially decreases linearly in μ , reflecting the linear decrease of the required energy to add a single particle in the system. When it is closer to zero, however, the value of ϵ_\pm approaches more slowly to zero,

especially for a smaller system. When we fit the decrease by a function of the shape $\exp(-c|\mu - \mu_0|)$, the exponent c is roughly in proportion to the system size L . This also suggests that the modes corresponding to ϵ_{\pm} are spatially localized.

2. Detection of end Majorana fermions

From the eigenvector of H_{BdG} corresponding to the eigenvalue ϵ^+ , $(\mathbf{u}_{\uparrow}, \mathbf{u}_{\downarrow}, \mathbf{v}_{\uparrow}, \mathbf{v}_{\downarrow})^T$, we define the averaged separation from the system center

$$\sqrt{\langle x^2 \rangle} \equiv \sqrt{\left[\sum_{\sigma,l} (l - l_c)^2 |\mathbf{v}_{\sigma,l}|^2 \right] / \left[\sum_{\sigma,l} |\mathbf{v}_{\sigma,l}|^2 \right]}.$$

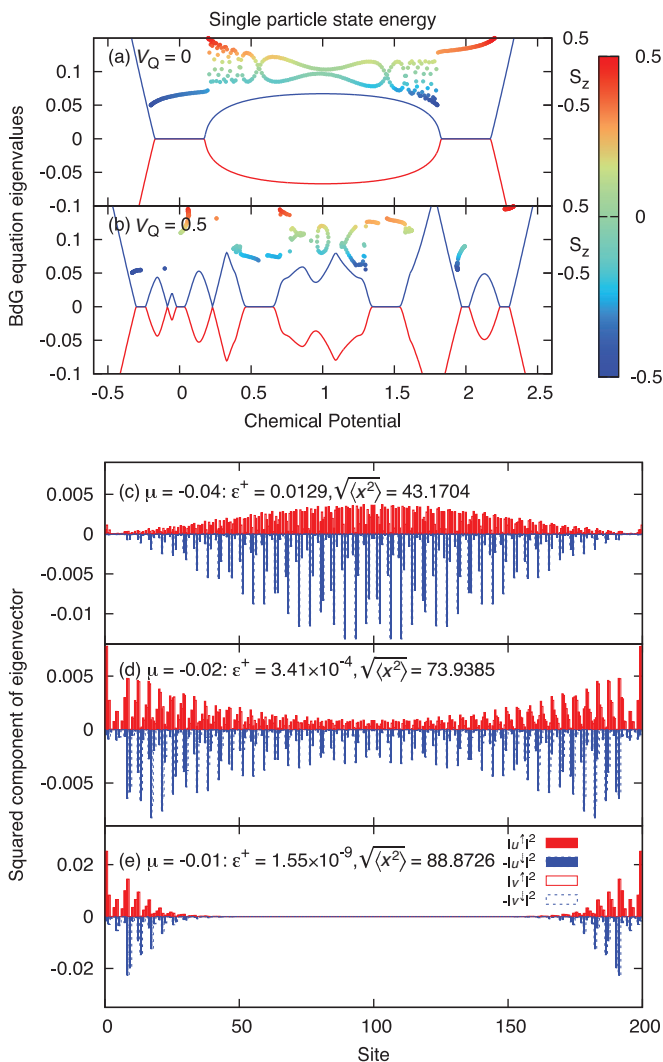


FIG. 2. (Color online) (a),(b) Largest negative (–) and smallest positive (+) eigenvalues of the BdG equation (5) plotted against the chemical potential μ for $g = \sqrt{5} - 2$, $(\Gamma, \alpha, \Delta) = (0.2, 0.3, 0.1)$, and (a) $V_Q = 0$, (b) $V_Q = 0.5$. Dots in the upper halves of the plots show the expectation value of the z component of the spin (right axis and color code) against the energy (top axis) for the single particle states of the nonsuperconducting version of the system, for the same sets of parameters except that Δ is set to zero. (c)–(e) Amplitudes of the particlelike and holelike parts of the eigenvectors $\sum_{\sigma} |u_{\sigma}|^2$, $\sum_{\sigma} |v_{\sigma}|^2$ plotted against the lattice site for $(\Gamma, \alpha, \Delta) = (0.2, 0.3, 0.1)$ and (c) $\mu = -0.04$, (d) $\mu = -0.02$, (e) $\mu = -0.01$.

If the modes localize to the system ends, $\sqrt{\langle x^2 \rangle}$ are close to l_c , the maximum value it can take. Note that, when ϵ^- and ϵ^+ are numerically degenerate ($\epsilon^+ \lesssim 10^{-12}$ in our work), any linear combination of the two eigenvectors that correspond to these eigenvalues would be obtained as the eigenvector corresponding to ϵ^+ , so within our BdG calculation we do not directly observe eigenmodes that are localized at only one of the ends of the system.

In the density-matrix renormalization group (DMRG) simulations of the same model,^{33,40} however, a pair of Majorana modes localized at each end of the system have been obtained. We believe that the DMRG calculation, with a limitation on the entanglement entropy between the two ends of the system, automatically chooses less entangled degenerate ground states, which are connected to each other by operating either of the two Majorana operators, for the subspaces with even and odd numbers of fermions. We find that the localization of $\mathbf{u}_{\sigma,l}$ and $\mathbf{v}_{\sigma,l}$, in terms of $\sqrt{\langle x^2 \rangle}$, precisely corresponds to the localization of the Majorana operators observed by DMRG.³³

We have plotted the values of ϵ^{\pm} as a function of μ along with the single particle state energy in Figs. 2(a) and 2(b). In Fig. 2(a) with $V_Q = 0$, the overlapping RZ bands are clearly observed, and ϵ^{\pm} vanish only when the chemical potential crosses only one of the RZ bands.

In Fig. 2(b) with $V_Q = 0.5$ several regions with vanishing ϵ^{\pm} are found, each corresponding to the energy region with states from just one of the two Hofstadter-butterfly-like structures. The components of the eigenvector corresponding to the eigenvalue ϵ^+ are shown in Figs. 2(c)–2(e) for values of μ approaching to one of the regions with vanishing ϵ^{\pm} . The localization of the mode is clearly observed with an increase of $\sqrt{\langle x^2 \rangle}$. In all regions with vanishing ϵ^{\pm} , we observe a clear localization of the corresponding eigenvectors of H_{BdG} .

C. Dependence on the lattice modulation wave number

In Ref. 33 we fixed the wave vector κ of the quasiperiodic lattice modulation. However, as we have observed in Fig. 1, we have effective single-band regions of the chemical potential for a wide range of the value of κ . Therefore it is interesting to study the dependence of the appearance of a topologically nontrivial superfluid with end Majorana fermions on the value of κ . Especially, it is intriguing whether a κ such that $2\pi/\kappa$ is an integer has any difference.

In Figs. 3 and 4 we plot the value of ϵ^+ in a color code, along with the single particle state energies obtained from Eq. (2). For smaller values of Δ , we notice that the vanishing eigenvalue corresponds to regions covered by a single band of single particle eigenstates, regardless of the value of κ . Particularly, even for values of κ such as $\pi/3$ and $\pi/2$, ϵ^+ vanishes when the chemical potential lies in the region where single particle eigenstates are effectively spinless.

In these regions, because of the effective single-band structure of the noninteracting Hamiltonian, the Kitaev model is realized, with Majorana fermion modes localizing at the system ends.³³ The value of ϵ^+ becomes closer to 0 as L is increased, reflecting that the end modes are more separated. For smaller L , the separation between the single particle eigenstates is comparable to Δ when $\Delta \ll \{\Gamma, t\}$. In this case,

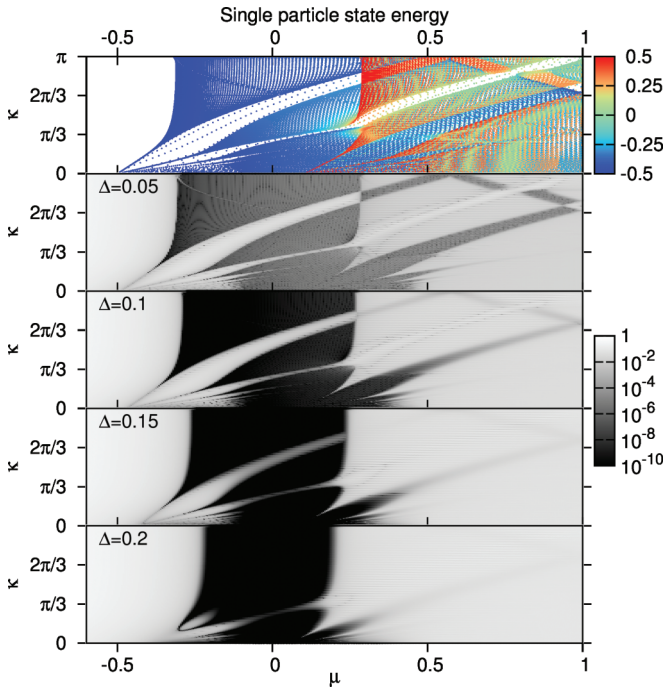


FIG. 3. (Color online) Top: Single particle eigenstates of Eq. (2) (nonsuperconducting case) color coded according to the value of S_z for $\hat{\mathbf{B}} = \hat{z}$, $L = 400$, $(\Gamma, \alpha, V_Q) = (0.3, 0.3, 0.2)$, and $0 < \kappa < \pi$. Lower: Grayscale plots of ϵ^+ for the same parameters with $\Delta = 0.05, 0.1, 0.15, 0.2$ and $-0.6 \leq \mu \leq 1$.

the strength of the induced superconductivity depends on the relative location of a level and the chemical potential. When the

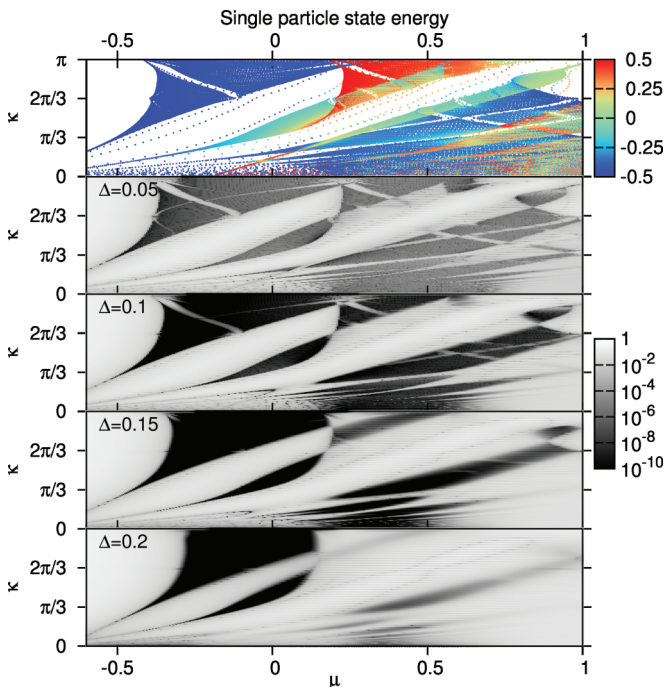


FIG. 4. (Color online) Top: Single particle eigenstates of Eq. (2) color coded according to the value of S_z for $\hat{\mathbf{B}} = \hat{z}$, $L = 400$, $(\Gamma, \alpha, V_Q) = (0.3, 0.3, 0.5)$, and $0 < \kappa < \pi$. Lower: Grayscale plots of ϵ^+ for the same parameters with $\Delta = 0.05, 0.1, 0.15, 0.2$ and $-0.6 \leq \mu \leq 1$.

separation is larger (the density of states is lower) the value of ϵ^+ usually stays larger, but changes rapidly. ϵ^+ becomes more homogeneous and generally reduced as Δ is increased inside each subband which does not overlap in energy with another.

We note that, while N_\downarrow is always larger than N_\uparrow for $\Gamma > 0$, there are subbands having fermions almost polarized in the $+\hat{z}$ direction ($\langle S_z \rangle \sim 1/2$) even when $\mu < 1$ with less than half filling factor ($N_\downarrow + N_\uparrow < L$). Remarkably, even when the chemical potential lies in one of such bands, a TS state with end Majorana fermions can be formed.

However, as Δ is increased, smaller features in the single particle state distribution, which remained in the structure of the value of ϵ^+ for smaller Δ , gradually disappear and only the widest single-band regions remain visible. A similar simplification of the phase diagram is also observed in Fig. 2 of Ref. 34 for a quasiperiodic system of spinless fermions. Finally, for $\Delta \gtrsim \Gamma$, the in-gap state disappears and the eigenvalue spectrum of H_{BdG} has a gap of the order of Δ , regardless of the value of V_Q , so that the system is topologically trivial.

In summary, the new topologically nontrivial regions with end Majorana fermions appear for general site energy modulations of the type of Eq. (4), and their existence is not limited to some special irrational values of $g = \kappa/(2\pi)$. The commensurate case can be considered as a kind of multiband wire. The possibility of TS states with end Majorana modes has also been studied in multiband systems.^{45–47} We have observed that while the range of the chemical potential strongly reflects the single particle eigenstate spectrum, the value of Δ also plays an important role. If Δ is too small ϵ^\pm vanishes only for regions with a higher density of states. If Δ is too large, smaller features in the single particle spectrum become smeared. This occurs before Δ exceeds Γ so that the system becomes topologically trivial regardless of the values of μ .

D. Dependence on the direction of the external magnetic field

The existence of the Majorana end fermions depends on the direction of the applied magnetic field.^{8–11} Namely, the effective magnetic field introduced by the Rashba spin-momentum coupling needs to have a perpendicular component to the external magnetic field. In our model the Rashba spin-momentum coupling is in the y direction, so the perpendicular directions lie in the z - x plane. Here we ask, can the spin-insensitive quasiperiodic modulation change this situation?

To answer this question we now consider $\hat{\mathbf{B}} = \hat{x} \cos \theta + \hat{y} \sin \theta$, with $0 \leq \theta \leq \pi/2$. We plot the value of ϵ^+ in a grayscale plot in Fig. 5(a). While the region with vanishing ϵ^+ persists up to $\theta \lesssim \pi/4$, which corresponds to $\Gamma_x \equiv \Gamma \cos \theta \gtrsim 0.2$, for larger θ with $\Gamma_x \lesssim 0.2$ we no longer have a vanishing eigenvalue of the BdG equation and the system is topologically nontrivial.

Therefore, the introduction of the site level modulation still does not lift the limitation in the direction of \mathbf{B} for TS states to be observed. Because $\Delta = 0.1$ still does not exceed Γ_x and the region with vanishing ϵ^+ is more fragile compared to the case with $V_Q = 0$ in Fig. 5(b), the result above indicates that the y component of the applied magnetic field is rather detrimental for the realization of a TS in our model.

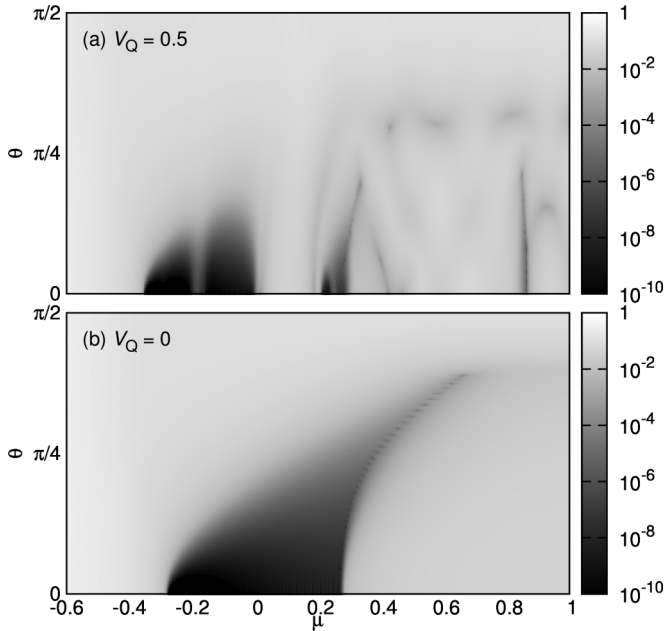


FIG. 5. Grayscale plot of the value of ϵ^+ for (a) $V_Q = 0.5$ and (b) $V_Q = 0$, $\hat{\mathbf{B}} = \hat{x} \cos \theta + \hat{y} \sin \theta$, $L = 200$, $(\Gamma, \alpha, \Delta) = (0.3, 0.3, 0.1)$, $g = (\sqrt{5} - 1)/2$, and $-0.6 \leq \mu \leq 1$, $0 \leq \theta \leq \pi/2$.

E. Dependence on the phase of the modulation potential

It has been known (see, e.g., Refs. 38 and 48–50) for systems with $\Gamma = \alpha = 0$ that when we fix the value of κ , one or more in-gap states emerge within the energy gaps due to the potential ϵ_l . Such in-gap states also exist in our model with nonzero Γ and α , and can cross each other or another subband because the RZ bands are shifted in energy. As we change the value of the phase of the site energy modulation ϕ_0 , the energies of these in-gap states change rapidly, while other states in “bulk” subbands do not change significantly.

In Fig. 6 we change the value of ϕ_0 to study the effect of such in-gap states. We have plotted the single particle state energies, color coded by the value of $\langle S_z \rangle$, as well as the value of ϵ^+ for different system sizes. The plot at the bottom with $L = 200$ looks similar to that of the single particle state energies at the top, except that the regions with two overlapping subbands do not have a vanishing ϵ^+ .

A quasiperiodic system is related by a Fourier transform to a periodic system with a gauge field in a higher spatial dimension,^{27,42} and the flow of the in-gap states as a function of ϕ_0 here corresponds to the existence of edge states in two-dimensional (2D) topological *insulators*.^{49–51} However, in our 1D system the quasiperiodicity coexists with topologically nontrivial *superconductivity*. Therefore it is not presently clear whether this flow, also appearing as a flow of narrow regions with vanishing ϵ^+ in the case with $\Delta > 0$, corresponds to the existence of a corresponding topological superconductivity in 2D. This is an interesting issue for future research.

We observe that the dependence of the eigenvalues on the choice of the phase ϕ_0 becomes weaker as L increases. Bulk subbands are not shifted, and crossing with a single in-gap state does not usually break the effective single-band situation. Therefore the topological equivalence between systems with different modulation phases is clear. In the next section we

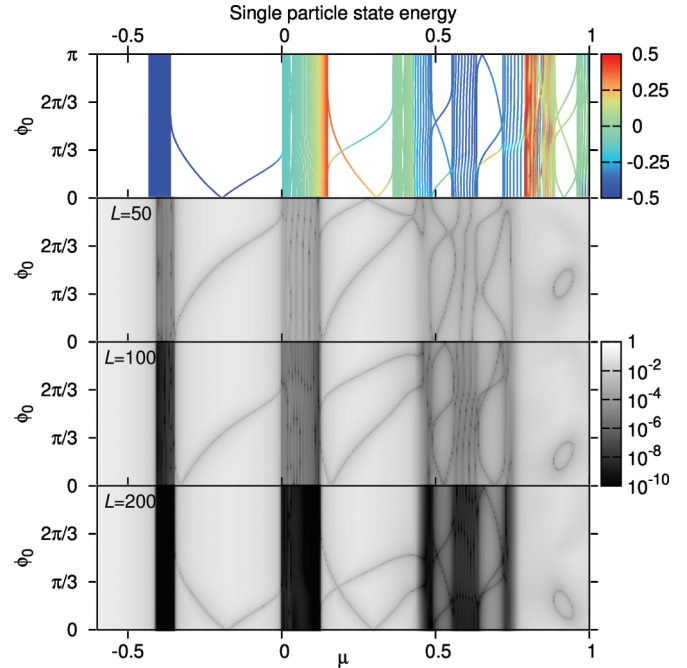


FIG. 6. (Color online) Top: Single particle eigenstates of Eq. (2) color coded according to the value of S_z for $g = \sqrt{5} - 2$, $\hat{\mathbf{B}} = \hat{z}$, $L = 200$, $(\Gamma, \alpha, V_Q) = (0.3, 0.3, 0.5)$, and $0 \leq \phi_0 \leq \pi$. Lower: Grayscale plots of ϵ^+ for the same set of parameters except that $\Delta = 0.1$ and $-0.6 \leq \mu \leq 1$ are introduced and $L = 50, 100, 200$.

study what happens if the modulation phase abruptly changes inside the quantum wire, or if the modulation disappears from a part of the wire.

III. EFFECTS OF DIFFERENT TYPES OF LATTICE MODULATION

A. Effect of phase jumps

In applications to the quantum information field, namely, quantum computation utilizing the pair annihilation or creation of multiple Majorana fermions via gates,⁵² end Majorana fermions should be stable against minor changes of the condition of the internals of the one-dimensional system, which would occur when two or more quantum wires are joined via gates. Our model of modulated lattices is characterized by the pair of the wave number κ and the phase ϕ_0 . Here, it is of much interest what happens if we have phase jumps of the lattice modulation, which would correspond to joints between quantum wires, in our system.

Let us consider a system with N_J phase jumps,

$$\epsilon_l = V_Q \cos[\kappa(l - l_c) + \phi_0 + \lfloor l/W \rfloor \phi_J], \quad (9)$$

in which $\lfloor x \rfloor$ denotes the largest integer not exceeding x and $W = L/(N_J + 1)$ is the distance between phase jumps of ϕ_J . If the phase jumps do not affect the Majorana modes, the regions of μ with vanishing ϵ^\pm should not change, and when they vanish, the corresponding eigenmodes should occupy the ends of the system in spite of the internal phase jumps.

In Fig. 7 we plot the value of ϵ^+ for (a) a single jump with different sizes of phase jump ϕ_J , and (b) different numbers of

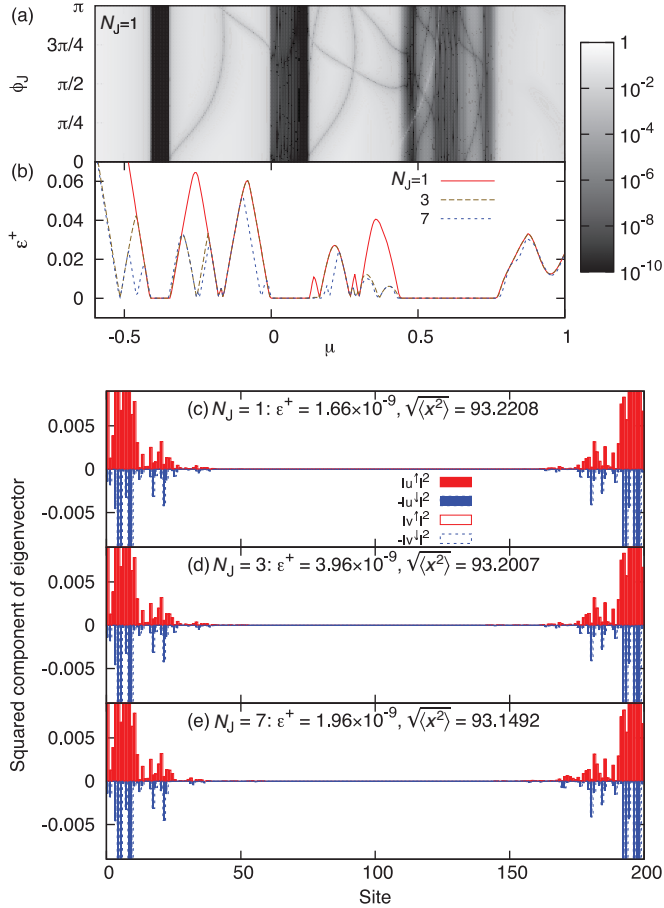


FIG. 7. (Color online) (a) Grayscale plots of ϵ^+ for $g = \sqrt{5} - 2$, $\hat{B} = \hat{z}$, $L = 200$, $(\Gamma, \alpha, V_Q) = (0.3, 0.3, 0.5)$, $\Delta = 0.1$, $-0.6 \leq \mu \leq 1$, $N_J = 1$, and $0 \leq \phi_J \leq \pi$. (b) Value of ϵ^+ plotted against μ for $N_J = 1, 3, 7$ and $\phi_J = \pi$. Eigenstates for $\mu = 0.04$ are plotted for (c) $N_J = 1$, (d) $N_J = 3$, and (e) $N_J = 7$.

phase jumps with $\phi_J = \pi$. In Fig. 7(a), $\phi_J = 0$ corresponds to a system without a phase jump. Introduction of a single phase jump almost does not change the locations of the regions with vanishing ϵ^\pm , though we observe a few curves of kinks in ϵ^+ corresponding to a single particle state running between RZ bands as ϕ_J is changed, in a way similar to what we have observed in Fig. 6. Increasing the number of phase jumps does not change the picture significantly, as long as the localization of the end modes is almost within a single section between phase jumps. This is observed in Fig. 7(b); while the values of ϵ^+ sometime differ between systems with different numbers of phase jumps of π , the regions with $\epsilon^+ \ll 1$ are not shifted or removed. Also we find in Figs. 7(c)–7(e) that the eigenvalues of H_{BdG} other than ϵ^\pm do not vanish in this case. There is only one pair of Majorana fermions appearing at the both ends of the system, rather than more than one pairs of them appearing also at phase jumps.

The results above reflect the fact that a phase jump does not change the topological character of the system. If both sides of the introduced phase jump are in the state characterized by the same topological quantum number, boundary states do not form at the phase jump.

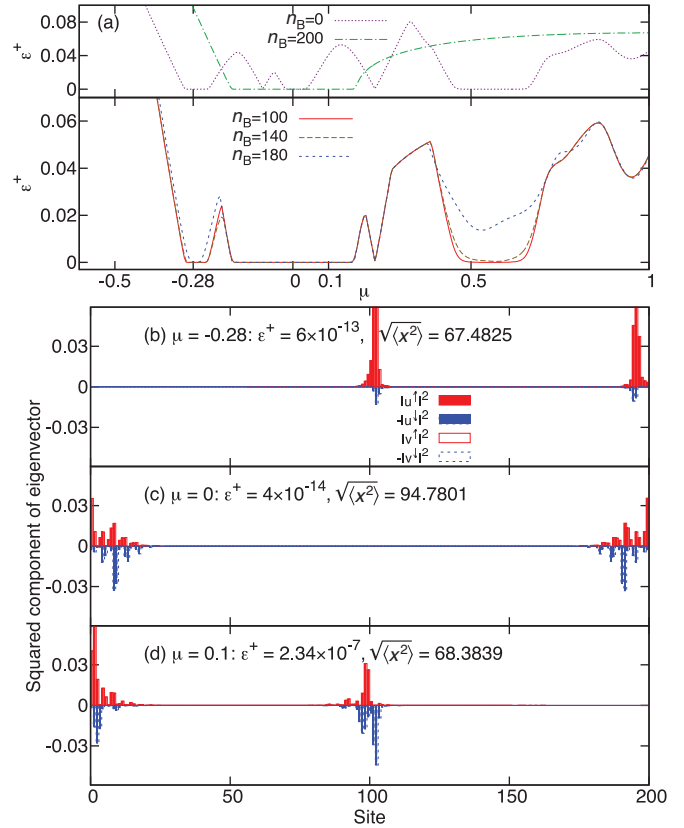


FIG. 8. (Color online) (a) Value of ϵ^+ plotted against μ for $n_B = 0, 200$ (upper panel) and for $n_B = 100, 140, 180$ (lower panel) and $g = \sqrt{5} - 2$, $\hat{B} = \hat{z}$, $L = 200$, $(\Gamma, \alpha, V_Q) = (0.2, 0.3, 0.5)$, $\Delta = 0.1$. Eigenstates for $n_B = 100$ are plotted for (b) $\mu = -0.28$ (only the right side of the system is single band), (c) $\mu = 0$ (both sides are single band), and (d) $\mu = 0.1$ (only the left side is single band).

B. Site level modulation limited to a part of the system

The view above is further confirmed when we remove the lattice modulation from some part of the system, by having

$$\epsilon_l = \begin{cases} 0 & (0 \leq l < n_B), \\ V_Q \cos[\kappa(l - l_c)] & (n_B \leq l < L). \end{cases} \quad (10)$$

In the lower panel of Fig. 8(a) we plot the value of ϵ^+ for different values of n_B for the case in which the part of the system to the left of site n_B has the same parameter as in Fig. 2(a) [plotted again in the upper panel of Fig. 8(a) as $n_B = 200$], whereas the right part has the same parameter as in Fig. 2(b) (plotted again in the upper panel as $n_B = 0$). For $n_B = L/2 = 100$ we observe that ϵ^+ vanishes when it vanishes either in Fig. 2(a) with $V_Q = 0$ or in Fig. 2(b) with $V_Q = 0.5$. In Figs. 8(b)–8(d) we have plotted the spatial distribution of eigenvectors of (5) corresponding to ϵ^+ . In Fig. 8(b) with $\mu = -0.28$, only the right side of the system with $V_Q = 0.5$ is an effective single-band system at the chemical potential and becomes a topological superconductor. The eigenvector has most of its amplitude localized equally to the two ends of this region, and the value of $\sqrt{\langle x^2 \rangle}$ is close to $L/(2\sqrt{2})$, as expected in such a case. Also, in Fig. 8(d) with $\mu = 0.1$, only the left side of the system without the lattice modulation becomes a topological superconductor, and the eigenvector is

this time localized to the two ends of the left part, with the value of $\sqrt{\langle x^2 \rangle}$ similar to that in Fig. 8(b). On the other hand, in Fig. 8(c) both sides are topologically nontrivial, and the eigenvector has its amplitudes localized at the two ends of the whole system.

As we enlarge the part without lattice modulation by increasing the value of n_B in the lower panel of Fig. 8(a), the plot of ϵ^+ approaches that in Fig. 2(a). This is because the part with the lattice modulation with $L - n_B$ sites cannot form a well-defined topological superconductor if it is too short.

In summary, when two TS regions are joined, the resulting system become a TS with end Majorana states at the ends. On the other hand, if a TS is joined with a topologically trivial chain, the resulting system becomes a TS whose Majorana states appear close to where they had been in the original TS. This does not depend on which of the chains has spatial modulation. If the chemical potential can be controlled in the system, one can control which region has boundary Majorana modes in the setting above.

C. Case of a hopping modulation

The correspondence between the ‘‘diagonal’’ modulation in the lattice-site energy and the ‘‘off-diagonal’’ one in the hopping amplitude in quasiperiodic systems has attracted a renewed attention.^{48,53} Here we study the effect of such a modulation in the hopping amplitude in our system, in which case the Hamiltonian is given by

$$\begin{aligned} \mathcal{H} = & - \sum_{l=0}^{L-2} \frac{t_l}{2} \sum_{\sigma=\uparrow,\downarrow} (\hat{c}_{\sigma,l}^\dagger \hat{c}_{\sigma,l+1} + \text{H.c.}) \\ & + \frac{\alpha}{2} \sum_{l=0}^{L-2} [(\hat{c}_{\downarrow,l}^\dagger \hat{c}_{\uparrow,l+1} - \hat{c}_{\uparrow,l}^\dagger \hat{c}_{\downarrow,l+1}) + \text{H.c.}] \\ & + \sum_{l=0}^{L-1} \left[\Delta (\hat{c}_{\uparrow,l} \hat{c}_{\downarrow,l} + \text{H.c.}) \right. \\ & \left. + \frac{2\Gamma}{\hbar} \hat{\mathbf{B}} \cdot \mathbf{S}_l + \sum_{\sigma=\uparrow,\downarrow} (t - \mu) \hat{n}_{\sigma,l} \right], \end{aligned} \quad (11)$$

with

$$t_l = t \{1 + V_J \cos[\kappa(l + 1/2 - l_c) + \phi_0]\}. \quad (12)$$

In Fig. 9 we plot the single particle state energy as well as the value of ϵ^+ obtained by solving the BdG equation similar to (5) but the diagonal (spin-preserving) blocks of the kinetic term substituted by the one with the modulated hopping parameter. We observe that, while the details of the single particle spectrum are changed, the correspondence between the effective single-band region in the spectrum and the zeros of the ϵ^+ is also observed here.

The symmetry of the Hamiltonian is not changed by going from the site level modulation to the hopping parameter modulation. Therefore a similar response to phase jumps or partial modulations inside the system is expected for the latter case as in the former case, which has been studied above.

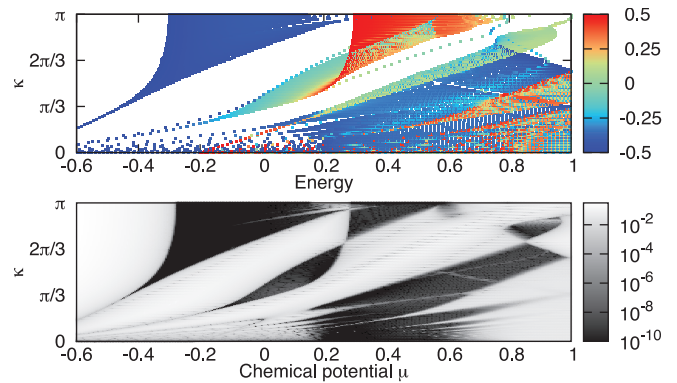


FIG. 9. (Color online) Effect of quasiperiodic modulation of the hopping parameter. Top: Single particle state energy for the single particle Hamiltonian obtained by setting $\Delta = \mu = 0$ in Eq. (11), with $\hat{\mathbf{B}} = \hat{\mathbf{z}}$, $L = 200$, $(\Gamma, \alpha, V_J) = (0.3, 0.3, 0.5)$, and $0 \leq \kappa \leq \pi$. Bottom: ϵ^+ calculated for Eq. (11) with the same set of parameters except that $\Delta = 0.1$ and $-0.6 \leq \mu \leq 1$ are introduced.

IV. CONCLUSION

In summary, we have studied the effect of different types of spatial modulations on the realization of a topological superconductor in a 1D conductor with proximity-induced superfluidity and spin-orbit coupling, extending our previous work, Ref. 33.

The combination of a quasiperiodic site energy modulation with the external Zeeman field and the spin-orbit coupling results in a single particle state energy distribution having a fractal pattern, called the *double Hofstadter butterfly*. Within the mean-field, Bogoliubov–de Gennes approximation, our model Hamiltonian can be diagonalized. We have demonstrated that the smallest positive eigenvalue of the Hamiltonian is strongly governed by the single particle energy spectrum for relatively weak induced superfluidity. Localized end modes, which are Majorana fermions, exist when two eigenvalues are degenerate at zero energy. As we change the chemical potential or the modulation wave number, we observe multiple reentrant transitions into and out of topologically nontrivial states. However, for stronger superfluidity, small patterns of the double Hofstadter butterfly are smeared from the eigenvalue plot showing the topologically nontrivial parameter ranges. The resulting topological superconductor is sensitive to the direction of the magnetic field, while the phase of the modulation does not affect the system.

We have also studied the effects of the phase jump of the quasiperiodic potential and what happens when the potential is applied to only a part of the quantum wire. The results reflect that the system is characterized by a Z_2 quantum number, that is, all the topologically nontrivial states are indistinguishable, and if two regions with such states are joined, the Majorana end modes appear only at the ends of the resulting system. If the chemical potential can be changed, the locations of the end modes can be manipulated. A quasiperiodic hopping modulation also exhibits a similar phase diagram with reentrant topological transitions.

Recently a scheme for topological superconductivity without a proximity effect has been proposed.⁵⁴ Our study of the correlation between the band structure and realization of

topological superconductivity could also be relevant in such cases.

ACKNOWLEDGMENTS

M.T. acknowledges the hospitality of Cavendish Laboratory, University of Cambridge, where this work was completed. This work was partially supported by the Grant-in-Aid for the

Global COE Program “The Next Generation of Physics, Spun from Universality and Emergence” from MEXT of Japan. N.K. is supported by KAKENHI (Grants No. 22103005 and No. 25400366) and JSPS through its FIRST Program. Part of the computation in this work has been performed using the facilities of the Supercomputer Center, Institute for Solid State Physics, University of Tokyo and Yukawa Institute for Theoretical Physics, Kyoto University.

*tezuka@sphys.kyoto-u.ac.jp

- ¹N. Read and D. Green, *Phys. Rev. B* **61**, 10267 (2000).
- ²A. Yu. Kitaev, *Phys.-Usp.* **44**, 268 (2001).
- ³D. A. Ivanov, *Phys. Rev. Lett.* **86**, 268 (2001).
- ⁴L. Fu and C. L. Kane, *Phys. Rev. Lett.* **100**, 096407 (2008).
- ⁵S. Fujimoto, *Phys. Rev. B* **77**, 220501 (2008); M. Sato and S. Fujimoto, *ibid.* **79**, 094504 (2009).
- ⁶M. Sato, Y. Takahashi, and S. Fujimoto, *Phys. Rev. Lett.* **103**, 020401 (2009).
- ⁷Y. Tanaka, T. Yokoyama, and N. Nagaosa, *Phys. Rev. Lett.* **103**, 107002 (2009); J. Linder, Y. Tanaka, T. Yokoyama, A. Sudbø, and N. Nagaosa, *ibid.* **104**, 067001 (2010).
- ⁸J. D. Sau, R. M. Lutchyn, S. Tewari, and S. Das Sarma, *Phys. Rev. Lett.* **104**, 040502 (2010).
- ⁹J. Alicea, *Phys. Rev. B* **81**, 125318 (2010).
- ¹⁰R. M. Lutchyn, J. D. Sau, and S. Das Sarma, *Phys. Rev. Lett.* **105**, 077001 (2010).
- ¹¹Y. Oreg, G. Refael, and F. von Oppen, *Phys. Rev. Lett.* **105**, 177002 (2010).
- ¹²S. Nakosai, Y. Tanaka, and N. Nagaosa, *Phys. Rev. Lett.* **108**, 147003 (2012).
- ¹³V. Mourik, K. Zuo, S. M. Frolov, S. R. Plissard, E. P. A. M. Bakkers, and L. P. Kouwenhoven, *Science* **336**, 1003 (2012).
- ¹⁴J. G. Rodrigo, V. Crespo, H. Suderow, S. Vieira, and F. Guinea, *Phys. Rev. Lett.* **109**, 237003 (2012).
- ¹⁵M. T. Deng, C. L. Yu, G. Y. Huang, M. Larsson, P. Caroff, and H. Q. Xu, *Nano Lett.* **12**, 6414 (2012).
- ¹⁶L. P. Rokhinson, X. Liu, and J. K. Furdyna, *Nat. Phys.* **8**, 795 (2012).
- ¹⁷T. D. Stanescu and S. Tewari, *J. Phys.: Condens. Matter* **25**, 233201 (2013).
- ¹⁸O. Motrunich, K. Damle, and D. A. Huse, *Phys. Rev. B* **63**, 224204 (2001).
- ¹⁹I. A. Gruzberg, N. Read, and S. Vishveshwara, *Phys. Rev. B* **71**, 245124 (2005).
- ²⁰P. W. Brouwer, M. Duckheim, A. Romito, and F. von Oppen, *Phys. Rev. Lett.* **107**, 196804 (2011); *Phys. Rev. B* **84**, 144526 (2011).
- ²¹R. M. Lutchyn, T. D. Stanescu, and S. Das Sarma, *Phys. Rev. B* **85**, 140513(R) (2012).
- ²²A. M. Lobos, R. M. Lutchyn, and S. Das Sarma, *Phys. Rev. Lett.* **109**, 146403 (2012).
- ²³D. Bagrets and A. Altland, *Phys. Rev. Lett.* **109**, 227005 (2012); P. Neven, D. Bagrets, and A. Altland, *New J. Phys.* **15**, 055019 (2013).
- ²⁴S. Takei, B. M. Fregoso, H. Y. Hui, A. M. Lobos, and S. Das Sarma, *Phys. Rev. Lett.* **110**, 186803 (2013).
- ²⁵İ. Adagideli, M. Wimmer, and A. Teker, [arXiv:1302.2612](https://arxiv.org/abs/1302.2612).
- ²⁶J. D. Sau, and S. Das Sarma, *Phys. Rev. B* **88**, 064506 (2013).
- ²⁷P. G. Harper, *Proc. Phys. Soc., London, Sect. A* **68**, 874 (1955).
- ²⁸G. Roati, C. D’Errico, L. Fallani, M. Fattori, C. Fort, M. Zaccanti, G. Modugno, M. Modugno, and M. Inguscio, *Nature (London)* **453**, 895 (2008); E. Lucioni, B. Deissler, L. Tanzi, G. Roati, M. Zaccanti, M. Modugno, M. Larcher, F. Dalfovo, M. Inguscio, and G. Modugno, *Phys. Rev. Lett.* **106**, 230403 (2011).
- ²⁹V. Brouet *et al.*, *Phys. Rev. B* **87**, 041106(R) (2013).
- ³⁰B. Hunt, J. D. Sanchez-Yamagishi, A. F. Young, M. Yankowitz, B. J. LeRoy, K. Watanabe, T. Taniguchi, P. Moon, M. Koshino, P. Jarillo-Herrero, and R. C. Ashoori, *Science* **340**, 1427 (2013).
- ³¹A. P. Schnyder, S. Ryu, A. Furusaki, and A. W. W. Ludwig, *Phys. Rev. B* **78**, 195125 (2008); A. Kitaev, *AIP Conf. Proc.* **1134**, 22 (2009).
- ³²M. Verbin, O. Zilberberg, Y. E. Kraus, Y. Lahini, and Y. Silberberg, *Phys. Rev. Lett.* **110**, 076403 (2013).
- ³³M. Tezuka and N. Kawakami, *Phys. Rev. B* **85**, 140508(R) (2012).
- ³⁴W. DeGottardi, D. Sen, and S. Vishveshwara, *Phys. Rev. Lett.* **110**, 146404 (2013).
- ³⁵X. Cai, L.-J. Lang, S. Chen, and Y. Wang, *Phys. Rev. Lett.* **110**, 176403 (2013).
- ³⁶I. Satija and G. G. Naumis, *Phys. Rev. B* **88**, 054204 (2013).
- ³⁷L.-J. Lang and S. Chen, *Phys. Rev. B* **86**, 205135 (2012).
- ³⁸S. Ganeshan, K. Sun, and S. Das Sarma, *Phys. Rev. Lett.* **110**, 180403 (2013).
- ³⁹J. Klinovaja, P. Stano, and D. Loss, *Phys. Rev. Lett.* **109**, 236801 (2012).
- ⁴⁰E. M. Stoudenmire, J. Alicea, O. A. Starykh, and M. P. A. Fisher, *Phys. Rev. B* **84**, 014503 (2011).
- ⁴¹M. Kohmoto, *Phys. Rev. Lett.* **51**, 1198 (1983); C. Tang and M. Kohmoto, *Phys. Rev. B* **34**, 2041 (1986).
- ⁴²D. R. Hofstadter, *Phys. Rev. B* **14**, 2239 (1976).
- ⁴³M. Iskin, *Phys. Rev. A* **85**, 013622 (2012).
- ⁴⁴X.-J. Liu, L. Jiang, H. Pu, and H. Hu, *Phys. Rev. A* **85**, 021603(R) (2012).
- ⁴⁵A. C. Potter and P. A. Lee, *Phys. Rev. Lett.* **105**, 227003 (2010); *Phys. Rev. B* **83**, 094525 (2011).
- ⁴⁶R. M. Lutchyn, T. D. Stanescu, and S. Das Sarma, *Phys. Rev. Lett.* **106**, 127001 (2011); T. D. Stanescu, R. M. Lutchyn, and S. Das Sarma, *Phys. Rev. B* **84**, 144522 (2011).
- ⁴⁷M.-T. Rieder, G. Kells, M. Duckheim, D. Meidan, and P. W. Brouwer, *Phys. Rev. B* **86**, 125423 (2012).
- ⁴⁸Y. E. Kraus and O. Zilberberg, *Phys. Rev. Lett.* **109**, 116404 (2012).
- ⁴⁹F. Mei, S.-L. Zhu, Z.-M. Zhang, C. H. Oh, and N. Goldman, *Phys. Rev. A* **85**, 013638 (2012).
- ⁵⁰L.-J. Lang, X. Cai, and S. Chen, *Phys. Rev. Lett.* **108**, 220401 (2012).
- ⁵¹Y. E. Kraus, Y. Lahini, Z. Ringel, M. Verbin, and O. Zilberberg, *Phys. Rev. Lett.* **109**, 106402 (2012).
- ⁵²L.-H. Wu, Q.-F. Liang, Z. Wang, and X. Hu, [arXiv:1302.3947](https://arxiv.org/abs/1302.3947).
- ⁵³S. Thiem and M. Schreiber, in *Aperiodic Crystals*, edited by S. Schmid, R. L. Withers, and R. Lifshitz (Springer, Netherlands, 2013), pp. 89–94.
- ⁵⁴A. Farrell and T. Pereg-Barnea, *Phys. Rev. B* **87**, 214517 (2013).